

Anisotropic conductivity of the Si(111)4 × 1-In surface: Transport mechanism determined by the temperature dependence

Tomoya Uetake, Toru Hirahara, Yoichi Ueda, Naoka Nagamura, Rei Hobara, and Shuji Hasegawa

Department of Physics, University of Tokyo, 7-3-1 Hongo, Bunkyo-ku, Tokyo 113-0033, Japan

(Received 17 May 2012; revised manuscript received 27 June 2012; published 26 July 2012)

The temperature dependence of anisotropic conductivity of a quasi-one-dimensional metallic surface, Si(111)4 × 1-In, was measured by a variable-temperature four-tip scanning tunneling microscope. Using the square four-point probe method, we succeeded in measuring the conductivity parallel and perpendicular to the In chains independently as a function of temperature. It was shown that the conductivity perpendicular to the In chains was mainly the conductivity of the space-charge layer of the substrate. Moreover, it was clarified that it strongly depends on the substrate flashing temperature and this sometimes hindered the anisotropic conductivity at low temperatures. In contrast, the conductivity parallel to In chains was clearly dominated by the surface states and decreased drastically around 110 K by the well-known 4 × 1 to 8 × 2 metal-insulator transition. The low temperature 8 × 2 phase had an energy gap as large as ~250 meV, consistent with previous photoemission reports.

DOI: [10.1103/PhysRevB.86.035325](https://doi.org/10.1103/PhysRevB.86.035325)

PACS number(s): 68.35.-p, 73.20.-r, 73.25.+i

I. INTRODUCTION

One-dimensional (1D) electron systems have been an area of active research since they show a variety of unusual physical properties,¹ such as the Tomonaga-Luttinger liquid,^{2,3} the spin-charge separation,⁴ and the formation of charge- or spin-density waves (CDW or SDW) due to the Peierls instability.^{5,6} A Si(111)4 × 1-In surface superstructure, composed of a massive array of metallic In atomic chains,⁷ is known to have quasi-1D metallic surface-state bands.⁸ It is found that a metal-insulator (MI) transition occurs in this system at about 120 K, where the 4 × 1 periodicity changes to the 8 × 2 phase.⁹ Initially it was suggested that the transition was driven by a (weak-coupling) Peierls instability.⁹ This was supported by other experimental evidences.^{10–12} However, other groups challenged this explanation based on calculations insisting that this transition was rather an order-disorder type.^{13,14} This actually is within the framework of a strong-coupling CDW transition.¹⁵ A detailed angle-resolved photoemission spectroscopy (ARPES) study showed that the band dispersions changed abruptly at around 120 K, producing a relatively large energy gap at E_F (~300 meV) compared to the energy scale of the transition temperature, which actually suggested that the CDW transition was not a weak-coupling type.¹⁶ It was found that the size of the gap showed a negligible temperature dependence, and proposed that the MI transition was caused by the cooperative effect of the Peierls and other structural transitions.¹⁶ A recent surface x-ray diffraction study proposed a very similar pseudo-first-order phase transition scenario.¹⁷ Density functional theory calculations combined with reflection anisotropy spectroscopy also show that this system undergoes a quasi-Peierls distortion with phonon softening.^{18,19} Thus, it seems that the origin of the MI transition in the quasi-1D indium chains on Si(111) surface is still a very intriguing topic and requires further experimental/theoretical studies for a consistent understanding of the phase transition (weak- or strong-coupling CDW or others).

Despite the above intricate debate, the Si(111)4 × 1-In surface is rather simple and, of course, interesting in terms of surface-state transport. Clear evidence of the MI transition

was found by temperature-dependent surface conductivity measurements using the linear micro-four-point-probe method (m4PP).²⁰ Furthermore, the anisotropic conductivity reflecting the quasi-1D band dispersion was directly measured with a four-tip scanning tunneling microscope (STM)²¹ using the rotational square m4PP method.²² However, there was one problem in the temperature-dependent transport data. In the linear m4PP, the obtained conductivity (σ) is the geometric mean of the conductivity parallel (σ_{\parallel}) and perpendicular (σ_{\perp}) to the In chains ($\sigma = \sqrt{\sigma_{\parallel}\sigma_{\perp}}$). Since there is evidence that σ_{\perp} is the space-charge-layer contribution,²⁴ we need to measure the temperature dependence of σ_{\parallel} and σ_{\perp} independently and unravel the actual transport mechanism of each channel to precisely discuss the surface-state transport. The previous measurements were performed with a four-tip STM that had no cooling capabilities.^{21,22} But we have recently developed a new machine which has the capability to cool down the sample and the tips.²⁵ Therefore in this paper, we have measured the conductivity of the Si(111)4 × 1-In surface using this machine with the square m4PP method and deduced the temperature dependence of σ_{\parallel} and σ_{\perp} independently. We found that the behavior of σ_{\perp} could be explained by the space-charge layer conductivity and showed significant change when we changed the substrate flashing temperature. On the other hand, we found that σ_{\parallel} was actually dominated by the surface-state conductivity as expected. It showed a MI transition around 110 K accompanying the 4 × 1 to 8 × 2 structural transition. The obtained gap size of the low temperature phase was ~250 meV, which was in accordance with that estimated from ARPES.¹⁶

II. EXPERIMENT

The conductivity measurements were performed with our custom-made variable-temperature four-tip STM system, in which the sample and tips were cooled down to 7 K in an ultrahigh vacuum (UHV).²⁵ Each probe made of a tungsten tip can be independently driven with piezoelectric actuators and a scanner in the x , y , and z directions to achieve precise positioning in nanometer scale under a scanning electron

microscope (SEM). The four-tip probes can be made to contact the sample surface in arbitrary arrangements, with marginal damage by the tunneling current approach and minute direct contact.

Vicinal Si wafers with 1–2° miscut from the (111) axis were used to grow a single-domain 4 × 1 phase. We used two types of substrates [*n*-type substrate (P doped) with a resistivity $\rho = 1\text{--}10\ \Omega\text{ cm}$ at room temperature (RT) and a nondoped substrate with a bulk resistivity $\rho \geq 1000\ \Omega\text{ cm}$ at RT] to study the effect of bulk conductivity on the measured conductivity. To obtain a single-domain 4 × 1 surface, a highly regular array of steps on Si(111) is needed, which can be formed by a multistep annealing sequence.²⁶ In this sequence the Si substrate is heated up to 1250 °C in UHV. However, Zhang *et al.* showed that such high temperature flashing caused the formation of a *p*-type layer near the surface region.²⁷ To avoid this, we also used a different way to clean the surface which was the Ishizaka-Shiraki method (chemical treating by HF etching in air and flashing up to 900 °C in UHV).²⁸ The Si(111)4 × 1-In surface was prepared by In deposition onto a cleaned Si(111)7 × 7 surface at 450 °C. The structural formation was monitored *in situ* during deposition by reflection high-energy electron diffraction (RHEED) observation.

III. RESULTS AND DISCUSSION

A. Anisotropic conductivity measurements at RT by the square m4PP method

Figure 1(a) shows current-voltage (*IV*) curves of a single domain Si(111)4 × 1-In surface measured by the square m4PP method. The probe spacing was 15 μm as shown by a SEM image at the left upper inset. The probes 1–4 are arranged in a square on the sample surface. The substrate for this data was flashed at 1250 °C to obtain a clean 7 × 7 surface. The blue open squares show the data points for the chain in the perpendicular (⊥) direction ($R_{\perp} = V_{43}/I_{12}$, which means that the current flows between probes 1 and 2 and the voltage drop between probes 3 and 4 is measured) and the red filled circles are those for the chain in the parallel (∥) direction ($R_{\parallel} = V_{23}/I_{14}$). The obtained resistance, which is the gradient of the *IV* curves, is $R_{\parallel} = 250 \pm 20\ \Omega$ and $R_{\perp} = 3.83 \pm 0.03\ \text{k}\Omega$, respectively, showing a large anisotropy as in the previous report.²²

This resistance can be converted into the conductivity in the following way. The resistance of an infinite two-dimensional (2D) layer/sheet measured in a square 4PP arrangement with equidistant probe spacing is given by

$$R_{\parallel} = \frac{1}{2\pi\sqrt{\sigma_{\parallel}\sigma_{\perp}}} \ln\left(1 + \frac{\sigma_{\perp}}{\sigma_{\parallel}}\right), \quad (1)$$

$$R_{\perp} = \frac{1}{2\pi\sqrt{\sigma_{\parallel}\sigma_{\perp}}} \ln\left(1 + \frac{\sigma_{\parallel}}{\sigma_{\perp}}\right), \quad (2)$$

where σ_{\parallel} and σ_{\perp} are the conductivities along and perpendicular to the In chains, respectively.^{22,29} By performing the simple algebra, $\sigma_{\parallel} = 220 \pm 10\ \mu\text{S}/\square$ and $\sigma_{\perp} = 32.7 \pm 0.4\ \mu\text{S}/\square$ are obtained. This clearly demonstrates the detection of the anisotropy in surface-state conductivity of a factor of 7. However, the ratio $\sigma_{\parallel}/\sigma_{\perp}$ depends on various factors as we will see below because the measured conductivity include

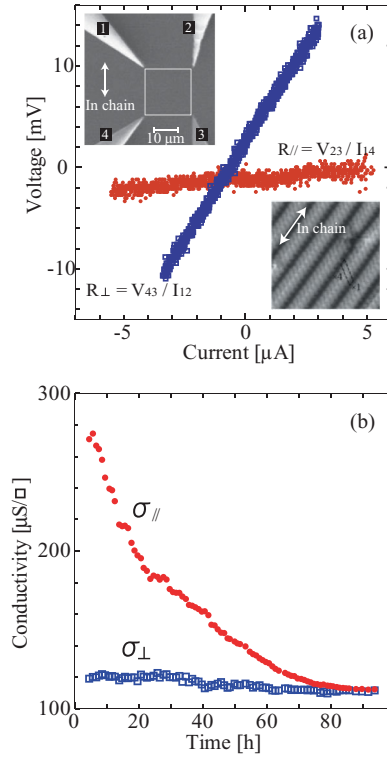


FIG. 1. (Color online) (a) *IV* curves of Si(111)4 × 1-In single domain measured by the square four-point probe method. Red filled circles and blue open square represent $R_{\parallel} = \frac{V_{23}}{I_{14}}$ and $R_{\perp} = \frac{V_{43}}{I_{12}}$, respectively. Upper left inset shows the SEM image of the tip arrangement. In chains are formed along the arrow, which is confirmed by the RHEED pattern. The right bottom inset shows STM image of Si(111)4 × 1-In. (b) Time dependence of conductivity of the Si(111)4 × 1-In surface. Red dots and blue open squares represent the obtained conductivity parallel (σ_{\parallel}) and perpendicular (σ_{\perp}) to the In chains.

the contribution from the underlying substrate and the space-charge layer conductivity which should be isotropic.²³

Figure 1(a) was taken 3 hours after the sample formation which was needed to cool down the sample back to RT. Figure 1(b) shows the time dependence of the measured conductivity. σ_{\perp} remains almost constant but σ_{\parallel} decreases drastically and the two become identical after 80 hours.³⁰ That is similar to the results of Okino *et al.*,²⁴ in which they measured the influence of defects on transport by intentionally exposing oxygen to the Si(111)4 × 1-In surface. This result shows that σ_{\parallel} is the sum of the surface-state conductivity σ_{SS} and the space-charge layer σ_{SCL} , and due to the disappearance of σ_{SS} by contamination, it decreases with time. On the other hand, σ_{\perp} remained almost constant even when the surface was contaminated by long-time exposure in a vacuum, which means that σ_{SCL} mainly contributes to σ_{\perp} . This will actually be supported by the discussion below. Summarizing, we can say that σ_{\parallel} and σ_{\perp} are

$$\sigma_{\parallel} = \sigma_{\text{SS}} + \sigma_{\text{SCL}}, \quad (3)$$

$$\sigma_{\perp} = \sigma_{\text{SCL}}, \quad (4)$$

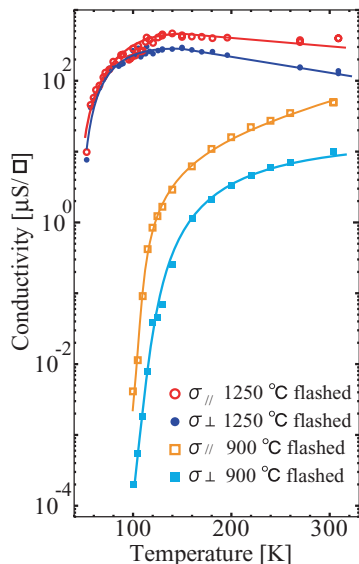


FIG. 2. (Color online) Temperature dependence of the anisotropic conductivity of Si(111)4 \times 1-In formed on the substrates flashed at 1250 °C and 900 °C (Ishizaka-Shiraki method). The solid lines are a guide for the eye.

respectively.³¹ It should be noted again that σ_{SS} is anisotropic due to the quasi-one-dimensional metallic surface-state bands, while σ_{SCL} is isotropic due to the bulk Si band structure.

B. Temperature dependence of the conductivity

Figure 2 shows the temperature dependence of the conductivity of the Si(111)4 \times 1-In surface. The 4 \times 1-In surface was prepared on nondoped Si(111) substrates which were flashed at 1250 °C or 900 °C (Ishizaka-Shiraki method) to obtain the 7 \times 7 surface. Because it took about 20 hours to cool down the sample in the four-tip STM, we should consider the temporal change of conductivity as shown above [Fig. 1(b)]. In the case of the sample flashed at 1250 °C, σ_{\perp} increases from RT to \sim 150 K showing a metallic behavior, and decreased drastically at lower temperatures (filled blue circles). The behavior for σ_{\parallel} is basically the same (red open circles), but we should note that although clear anisotropy was detected near RT, there is no difference between σ_{\parallel} and σ_{\perp} below about 100 K.

In the case of the samples flashed at 900 °C with the Ishizaka-Shiraki method, the values of both σ_{\perp} (cyan filled squares) and σ_{\parallel} (open orange squares) at RT were lower than the values of the sample flashed at 1250 °C by an order of magnitude and decreased as the temperature was cooled down. The decrease became significant below 140 K. Furthermore, the anisotropy remained even at low temperatures. Thus, the measured conductivity depends very much on the flashing temperature for surface cleaning.

Although we did the same measurements with different substrates (n -type P doped, bulk resistivity 1 \sim 10 Ω cm at RT), the measured values were in almost the same order even though the bulk resistivity differed by three orders of magnitude. This proves that the bulk does not contribute to these results and only the surface states (σ_{SS}) and space-charge layer (σ_{SCL}) conductivities are measured. Furthermore, the case of the n -type substrate also showed similar features as the

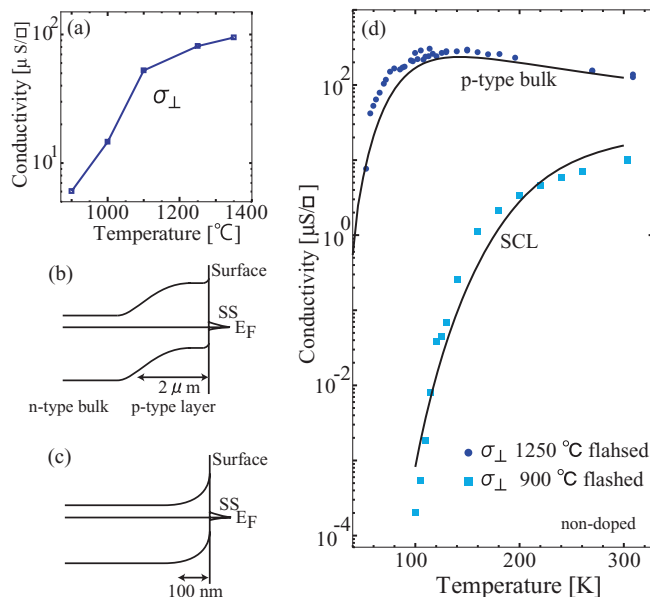


FIG. 3. (Color online) (a) Flashing temperature dependence of σ_{\perp} . (b), (c) Schematic drawing of band bending of the sample flashed at 1250 °C (b), and that flashed at 900 °C for an n -type sample (c). (d) Temperature dependence of σ_{\perp} for samples flashed at 1250 °C and 900 °C. Solid lines are calculated conductivity for p -type bulk and an inversion-type space-charge layer.

nondoped substrate; negligibly small anisotropy was shown at low temperature when flashed at 1250 °C while anisotropy was clearly detected for the sample flashed at 900 °C. These results suggest that the flashing at 1250 °C washed out the anisotropy in the surface-state conductivity by dramatically increasing the space-charge-layer conductivity.

1. Temperature dependence of σ_{\perp} : Conductivity of the space-charge (subsurface) layer

First we discuss the behavior of σ_{\perp} in more detail. From Fig. 2, we found that the values and temperature dependence of σ_{\perp} rely significantly on the flashing temperature for cleaning the substrates. To gain more insight into the relation between σ_{\perp} and the flashing temperature, we measured σ_{\perp} at RT as a function of the flashing temperature [Fig. 3(a)]. The values of σ_{\perp} increased systematically by increasing the flashing temperature and changed by an order of magnitude by going from 900 °C to 1350 °C. To interpret this, we recall the report by Zhang *et al.*²⁷ It is suggested that after high temperature flashing, a p -type layer is formed near the surface irrespective of the doping type of the substrate used as schematically shown in Fig. 3(b). Therefore in contrast to the simple band bending expected from the surface-core level shift [Fig. 3(c)], the conductivity of the space-charge layer can change by changing the flashing temperature. This was also confirmed from Hall effect measurements, which showed a p -type Hall resistance even when an n -type substrate was used.³²

Liehr *et al.* also reported that due to high temperature annealing in a vacuum, boron diffuses into the substrate to form an p -type layer near the surface.³³ According to their results, although the space-charge region of the Si substrate flashed at 1035 °C was around 100 nm below the surface, it

was deepened to more than $2 \mu\text{m}$ after annealed at 1300°C . Using these values, the estimated values of the conductivity (at RT) near the subsurface of the substrates annealed at 1035°C and 1300°C are $4 \mu\text{S}/\square$ and $200 \mu\text{S}/\square$, respectively. These values are in reasonable agreement with our measured results of σ_{\perp} for both the substrates flashed at 900°C and 1250°C . The reported amounts of dopant in the substrates annealed at high temperature is in the order of 10^{16}cm^{-3} , and the substrates annealed 1250°C in our experiment would be doped to the same order of magnitude in the subsurface region.

Now we turn to the temperature dependence of the conductivity in these space-charge layers. We assume that the heavily p -doped subsurface region in Fig. 3(b) should be considered as that of a p -type bulk of $\sim 2\text{-}\mu\text{m}$ thick.³⁵ Figure 3(d) shows the measured temperature dependence of σ_{\perp} and the calculated results of an inversion-type space-charge layer as shown by Fig. 3(c) for the 900°C -flashed sample (the surface Fermi level position of the 4×1 -In is 0.13 eV above the bulk valence-band maximum)²⁰ and a p -type bulk doped in the order of 10^{16}cm^{-3} for the 1250°C -flashed sample.³⁴ The calculated results agree almost completely with the experimental data. Generally, the conductivity can be written as

$$\sigma = en\mu, \quad (5)$$

where n is the carrier density, e is the elementary charge, and μ is the mobility. In the calculation, the carrier density for the $2 \mu\text{m}$ p -type bulk was derived assuming an acceptor concentration of 10^{16}cm^{-3} (Ref. 34). The temperature dependence arises from the Fermi-Dirac distribution function. The mobility also shows temperature dependence³⁴ and the metallic behavior from RT to $\sim 150 \text{ K}$ of the sample flashed at 1250°C can be explained by the increased mobility of carriers upon cooling. Because n is almost constant in this temperature region (saturation regime), σ reflects the behavior of μ . The drastic decrease of σ below 150 K reflects the freeze-out of n . This kind of behavior was actually reported by Morin *et al.*³⁶ On the other hand, for the usual inversion-type space-charge layer as shown in Fig. 3(c), using a well-established method by solving the Poisson's equation, we obtained the band bending and the resulting excess carrier concentration since the E_F positions at the surface and in the deep bulk are known. The decrease of n happens from RT and σ_{SCL} decreases already from RT as in the case of σ_{\perp} at 900°C flashed sample in Fig. 3(d).

2. Temperature dependence of σ_{\parallel} : Surface-state conductivity

All of the above facts showed that σ_{\perp} is dominated by the conductivity of the space-charge layer or the subsurface region (σ_{SCL}) as indicated in Eq. (4), meaning a negligible contribution from σ_{SS} . Now we move on to discuss σ_{\parallel} . As written in Eq. (3), σ_{\parallel} should be the sum of σ_{SS} and σ_{SCL} . Since σ_{SCL} is equal to σ_{\perp} , we can also estimate σ_{SS} by subtracting σ_{\perp} from σ_{\parallel} ($\sigma_{\text{SS}} = \sigma_{\parallel} - \sigma_{\text{SCL}}$).

Figure 4(a) shows the temperature dependence of σ_{SS} thus obtained for samples prepared differently (also with different bulk doping) which actually showed anisotropy at low temperature. Shown together is the temperature dependence of the RHEED spot intensity of the $\times 2$ streaks [marked by a rectangle in Fig. 4(b)]. The $\times 2$ spots began appearing around

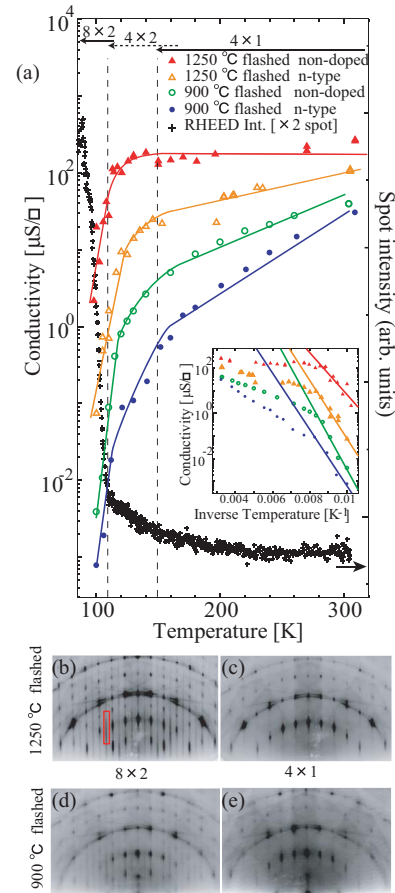


FIG. 4. (Color online) (a) The temperature dependence of the surface-state conductivity σ_{SS} for samples prepared at different flashing temperatures and the RHEED spot intensity of the $\times 2$ spot. Curved lines are a guide for the eye. (Inset) Arrhenius plot of σ_{SS} . Solid lines are fitted lines to $\sigma \propto \exp(-\frac{\Delta}{k_{\text{B}}T})$. (b) 8×2 and (c) 4×1 RHEED patterns of the sample flashed at 1250°C . (d) 8×2 and (e) 4×1 RHEED patterns of the sample flashed at 900°C .

150 K , meaning a periodicity doubling along the In chains. There was no indication of the $\times 8$ spots at this temperature, meaning that there is no correlation of this intrachain doubling between the neighboring chains. Then the $\times 2$ spot intensity drastically increased at 110 K with the appearance of the $\times 8$ spot. As for the σ_{SS} , although we see some differences, all the samples basically show the same behavior: σ_{SS} slightly decreases from RT down to $\sim 150 \text{ K}$, then the slope of the decrease becomes slightly larger below 150 K , then finally it drastically decreases at 110 K which corresponds to the phase transition to the 8×2 phase. Therefore, the origin of the drastic decreasing behavior of σ_{SS} below 110 K can be attributed to the occurrence of the MI transition reported previously.²⁰ Also, the change in the decrease speed at 150 K can be related to the appearance of the 4×2 phase. Because the 4×2 structure appears around defects and the 4×1 and 4×2 phases are coexisting with the domain walls fluctuating before the appearance of the $\times 8$ spots,¹² there are still conductive percolation paths above 110 K . Therefore the slight increase in the decrease rate of σ_{SS} around 150 K is likely due to the

$4 \times 1 \rightarrow 4 \times 2$ transition. Below 110 K, such conductive percolation paths are closed by the 8×2 phase formation.

It is possible to deduce the energy gap (2Δ) in the insulating 8×2 phase from the equation, $\sigma_{SS} \propto \exp(-\frac{\Delta}{k_{BT}})$. The inset in Fig. 4(a) shows the results fitted to $\ln \sigma_{SS} \propto 1/T$ which gives $2\Delta = 250 \pm 30$ meV. This is consistent with the gap observed in ARPES measurements (200, 80, and 340 meV for the $m1$, $m2$, and $m3$ bands, respectively).¹⁶ This reconfirms that we are actually measuring the surface-state conductivity in these measurements.

However, there is one discrepancy between the present surface-state conductivity and previous ARPES measurements. In our measurement, the temperature dependence of σ_{SS} in the 4×1 phase is nonmetallic (σ_{SS} decreases with cooling) in contrast to the metallic band structure above the MI transition temperature. The nonmetallic behavior can be especially noticed in the samples flashed at 900 °C. As we have mentioned before, the values of σ_{SS} of the sample flashed at 900 °C is lower than that of the samples flashed at 1250 °C by almost an order of magnitude. This is probably because of the defective surface, which hinders metallic conduction and lowers the conductivity itself. As discussed in Ref. 37, when the sheet conductivity is roughly below the minimum metallic conductivity ($2e^2/h \cong 80 \mu\text{S}/\square$), the temperature dependence becomes nonmetallic. The Si(111)- 7×7 and Si(111)- $\sqrt{3} \times \sqrt{3}$ -Sn surfaces are other examples of this.^{38,39} Figures 4(b) and 4(c) show the RHEED patterns of Si(111) 8×2 -In and 4×1 of the substrates flashed at 1250 °C, whereas Figs. 4(d) and 4(e) are those for samples flashed at 900 °C after Ishizaka-Shiraki etching. The patterns for the 900 °C flashed samples are much weaker and more blurred than those of the 1250 °C flashed ones, showing lower surface quality. Another reason may be that the defect density increased upon cooling since it took about 8–10 hours to cool down the sample to 150 K, which was much longer than the case of a monolithic m4PP machine in Ref. 20. According to Fig. 1(b), the surface-state conductivity is decreased by 40% in 10 hours. Thus, such

a defect increase may be responsible for the nonmetallic conduction in the 4×1 phase.

One may also notice that the phase transition has been somehow blurred and the transition temperature seems to be increased for the samples flashed at 900 °C. This is likely another effect of defects on the surface. It has been shown previously that inducing O/H defects on this system makes the transition less apparent and the phase transition temperature determined by the conductivity measurements increases due to the pinning effect of the $\times 2$ fluctuation by the defects.⁴⁰

IV. CONCLUSION

In summary, we measured the temperature dependence of anisotropic surface-state conductivity of Si(111) 4×1 -In using the variable-temperature four-tip STM. By the square m4PP method, we succeeded in measuring the conductivity parallel and perpendicular to In chains independently as a function of temperature and clarified the transport mechanism. We have found that the conductivity perpendicular to the In chains σ_{\perp} is mainly the conductivity of the space-charge layer of the substrate σ_{SCL} . Moreover, it was verified that σ_{SCL} strongly depended on the flashing temperature of the substrate, probably because of boron incorporation. In contrast, the conductivity parallel to In chains σ_{\parallel} is mainly dominated by the surface states. The σ_{SS} decreased drastically at 110 K due to the well-known metal-insulator transition. The LT phase (8×2) had an energy gap as large as ~ 250 meV, consistent with previous ARPES measurements.¹⁶ However, the expected metallic behavior at the high-temperature phase was not detected probably due to defects on the surface.

ACKNOWLEDGMENTS

This work has been supported by Grants-In-Aid from the Japan Society for the Promotion of Science and Japan Science and Technology Agency.

¹S. Hasegawa, *J. Phys.: Condens. Matter* **22**, 084206 (2010).

²J. M. Luttinger, *J. Math. Phys.* **4**, 1154 (1963).

³C. Blumstein, J. Schäfer, S. Mietke, S. Meyer, A. Dollinger, M. Lochner, X. Y. Cui, L. Patthey, R. Matzdorf, and R. Claessen, *Nat. Phys.* **7**, 776 (2011).

⁴E. H. Lieb and F. Y. Wu, *Phys. Rev. Lett.* **20**, 1445 (1968).

⁵R. E. Peierls, *Quantum Theory of Solids* (Clarendon, Oxford, 1964).

⁶T. Aruga, *J. Phys.: Condens. Matter* **14**, 8393 (2002).

⁷O. Bunk, G. Falkenberg, J. H. Zeysing, L. Lottermoser, R. L. Johnson, M. Nielsen, F. Berg-Rasmussen, J. Baker, and R. Feidenhansl, *Phys. Rev. B* **59**, 12228 (1999).

⁸T. Abukawa, M. Sasaki, F. Hisamatsu, T. Goto, T. Kinoshita, A. Kakizaki, and S. Kono, *Surf. Sci.* **325**, 33 (1995).

⁹H. W. Yeom, S. Takeda, E. Rotenberg, I. Matsuda, K. Horikoshi, J. Schaefer, C. M. Lee, S. D. Kevan, T. Ohta, T. Nagao, and S. Hasegawa, *Phys. Rev. Lett.* **82**, 4898 (1999).

¹⁰J. Guo, G. Lee, and E. W. Plummer, *Phys. Rev. Lett.* **95**, 046102 (2005).

¹¹G. Lee, J. Guo, and E. W. Plummer, *Phys. Rev. Lett.* **95**, 116103 (2005).

¹²S. J. Park, H. W. Yeom, J. R. Ahn, and I.-W. Lyo, *Phys. Rev. Lett.* **95**, 126102 (2005).

¹³C. González, F. Flores, and J. Ortega, *Phys. Rev. Lett.* **96**, 136101 (2006).

¹⁴C. González, J. Guo, J. Ortega, F. Flores, and H. H. Weitering, *Phys. Rev. Lett.* **102**, 115501 (2009).

¹⁵E. Tosatti, in *Electronic Surface and Interface States on Metallic Systems* (World Scientific, Singapore, 1995), p. 67.

¹⁶Y. J. Sun, S. Agario, S. Souma, K. Sugawara, Y. Tago, T. Sato, and T. Takahashi, *Phys. Rev. B* **77**, 125115 (2008).

¹⁷S. Hatta, Y. Ohtsubo, T. Aruga, S. Miyamoto, H. Okuyama, H. Tajiri, and O. Sakata, *Phys. Rev. B* **84**, 245321 (2011).

¹⁸W. G. Schmidt, S. Wippermann, S. Sanna, M. Bablioni, N. J. Vollmers, and U. Gerstmann, *Phys. Status Solidi B* **249**, 343 (2012).

¹⁹S. Chandola, K. Hinrichs, M. Gensch, N. Esser, S. Wippermann, W. G. Schmidt, F. Bechstedt, K. Fleischer, and J. F. McGill, *Phys. Rev. Lett.* **102**, 226805 (2009).

²⁰T. Tanikawa, I. Matsuda, T. Kanagawa, and S. Hasegawa, *Phys. Rev. Lett.* **93**, 016801 (2004).

- ²¹S. Hasegawa, I. Shiraki, F. Tanabe, and R. Hobar, *Current Appl. Phys.* **2**, 465 (2002).
- ²²T. Kanagawa, R. Hobar, I. Matsuda, T. Tanikawa, A. Natori, and S. Hasegawa, *Phys. Rev. Lett.* **91**, 036805 (2003).
- ²³We have previously reported a much higher value of anisotropy in Ref. 22. But since the value of σ_{\perp} depends significantly on the flashing temperature [Fig. 3(a)], the value of σ_{\parallel} is the real important parameter. As shown in Fig. 4(a), σ_{\parallel} is around 100 μS and is within the experimental error consistent with what was reported in Ref. 22.
- ²⁴H. Okino, I. Matsuda, R. Hobar, S. Hasegawa, Y. Kim, and G. Lee, *Phys. Rev. B* **76**, 195418 (2007).
- ²⁵R. Hobar, N. Nagamura, S. Hasegawa, I. Matsuda, Y. Yamamoto, K. Ishikawa, and T. Nagamura, *Rev. Sci. Instrum.* **78**, 053705 (2007).
- ²⁶J. Viernow, J.-L. Lin, D. Y. Petrovykh, F. M. Leibsle, F. K. Men, and F. J. Himpsel, *Appl. Phys. Lett.* **72**, 948 (1998).
- ²⁷H. M. Zhang, K. Sakamoto, G. V. Hansson, and R. I. G. Uhrberg, *Phys. Rev. B* **78**, 035318 (2008).
- ²⁸A. Ishizaka and Y. Shiraki, *J. Electrochem. Soc.* **133**, 666 (1986).
- ²⁹S. Hasegawa, *Chin. J. Phys.* **45**, 385 (2007).
- ³⁰To avoid contamination effects from the electron beam irradiation, the SEM observation was performed only during the measurements and was turned off while waiting in the measurement of Fig. 1(b). This was actually quite important and if we turned on the SEM at all times during the measurement, the decrease in σ_{\parallel} was much more rapid. When we measured the temperature dependence of the conductivity, the SEM was also turned on only during the measurement and was turned off while waiting for the sample to cool down. We only directly contacted the sample with the probes for the measurements and for the rest of the time, the contact was maintained as a tunneling contact.
- ³¹The bulk contribution can be neglected because of the small probe spacing and a pn junction between the surface space-charge layer and the bulk, which can be confirmed by changing the substrate doping level.
- ³²T. Hirahara, I. Matsuda, C. Liu, R. Hobar, S. Yoshimoto, and S. Hasegawa, *Phys. Rev. B* **73**, 235332 (2006).
- ³³M. Liehr, M. Renier, R. A. Wachnik, and G. S. Sciila, *J. Appl. Phys.* **61**, 4619 (1987).
- ³⁴S. M. Sze and K. K. Ng, *Physics of Semiconductor Devices*, 3rd ed. (John Wiley and Sons, New York, 2006).
- ³⁵We have shown in Ref. 20 that the metal-insulator transition cannot be measured by using a p -type substrate. This is because the current mainly flows through the bulk. But in the present case, although a p -type layer is formed in the space-charge region, the substrate itself is n type. Therefore, there is a carrier depletion layer which makes the current flow confined within the surface region.
- ³⁶F. J. Morin and J. P. Maita, *Phys. Rev.* **96**, 28 (1954).
- ³⁷S. Yamazaki, Y. Hosomura, I. Matsuda, R. Hobar, T. Eguchi, Y. Hasegawa, and S. Hasegawa, *Phys. Rev. Lett.* **106**, 116802 (2011).
- ³⁸M. D'angelo, K. Takase, N. Miyata, T. Hirahara, S. Hasegawa, A. Nishide, M. Ogawa, and I. Matsuda, *Phys. Rev. B* **79**, 035318 (2009); T. Tanikawa, K. Yoo, I. Matsuda, S. Hasegawa, and Y. Hasegawa, *ibid.* **68**, 113303 (2003).
- ³⁹T. Hirahara, T. Komorida, Y. Gu, F. Nakamura, H. Idzuchi, H. Morikawa, and S. Hasegawa, *Phys. Rev. B* **80**, 235419 (2009).
- ⁴⁰T. Shibusaki, N. Nagamura, T. Hirahara, H. Okino, S. Yamazaki, W. Lee, H. Shim, R. Hobar, I. Matsuda, G. S. Lee, and S. Hasegawa, *Phys. Rev. B* **81**, 035314 (2010).